Energy Proceedings
Vol 51, 2025
ISSN 2004-2965

Transient Behavior of a Two-phase-closed Geothermal Thermosyphon[#]

Tareen, M. S. K. [1,2], Badache, M. [2], & Sasmito, A. P. [1*]

1 CanmetENERGY – Natural Resources Canada, Varennes, QC, J3X 1P7, Canada

2 McGill University, Department of Mining and Materials Engineering, Montreal, QC, H3A 2A7, Canada
(Corresponding Author: agus.sasmito@mcgill.ca)

ABSTRACT

This study investigates the transient response of a novel CO_2 geothermal thermosyphon (GT) integrated with heat recovery ventilators (HRVs), used to reduce the heating load of buildings in northern regions. Particularly, the transient response of the GT-HRV test bench is presented in this paper, characterizing the integrated system response under various test conditions in terms of time constant (T), heat transfer rate, and average evaporator temperature (T_{ev}). Key experimental parameters include the GT filling ratio, coolant temperature, and coolant flow rate. The results indicate that a distinct T can be associated with each location of GT in fixed experimental conditions ranging from 417 seconds to 3762 seconds for coolant flow rate and inlet temperature set points of 0.05, 0.1, 0.15 and 0.2 l/s, and -9, -5 and -1 °C.

Keywords: Heat recovery ventilators, Geothermal thermosyphon, renewable energy, geothermal energy, energy systems, climate change

NONMENCLATURE

Abbreviations	
GT	Ground Thermosyphon
HRV	Heat recovery ventilator
ERV	Energy recovery ventilator
ES	Evaporator Section
TC	Thermocouple
PG	Propylene Glycol
FR	Filling ratio
HE	Heat exchanger
IA/EA	Incoming air
EA	Exhaust air
Symbols	
T	Time constant (sec)
T	Temperature (°C)
T_{ev}	Average evaporator temperature (°C)
Q	Heat transfer rate (kW)
Symbols	
ρ	Density (kg/m^3)
Cp	Specific heat (kJ/kg/K)
$\dot{m}$	Flow rate (l/s)
t	Time (sec)

1. INTRODUCTION

In an artificially heated building – for human comfort in extremely cold environments such as arctic climate – fresh air intake is critical to the well-being of its occupants. In Canadian winters, the fresh incoming air (IA) temperature can go lower than -40 °C. Heating the IA to room temperature is very energy intensive in such conditions. Thus, heat/energy recovery (HRV/ERV) technologies are installed to exchange heat between the IA and exhaust air (EA) to optimize energy use and to meet indoor air quality requirements in buildings.

Heat/energy recovery between the two air streams can be in the form of sensible or enthalpy heat recovery (Mardiana-Idayu et al. 2012) occurring in a heat exchanger (HE). For example, fixed plate, heat pipe, Rotary wheel, microchannel and run-around coil, etc. (Mardiana-Idayu et al. 2012). Metal based HEs can recover sensible heat while permeable fiber/polymer based HEs can also exchange latent heat (Mardiana et al. 2013).

A common problem in the operation of HRVs is frosting. It occurs because the temperature of the heat-exchange surface is below the freezing point and dew point of humid EA (Zhang et al. 2022). It commonly occurs when the average IA temperature is below -5 °C (also called as frosting limit) during the season (Rafati et al. 2014). Frost layer blocks the air passage and reduces heat transfer efficiency of HRV. Multiple frost detection and mitigation strategies are deployed and have additional energy cost (Bai et al. 2022). It is thus a concurrent research challenge to optimize energy consumption in building heating/ventilation operation in arctic climate – overcoming issues that affect the

This is a paper for the 16th International Conference on Applied Energy (ICAE2024), Sep. 1-5, 2024, Niigata, Japan.

efficiency of heat transfer devices, such as frost formation.

To further optimize the HRVs used in buildings in cold regions, an idea was proposed by Badache et al. (2024) recommending integration of HRVs with GT to utilize the geothermal energy available in the ground below the building of interest. A test bench was commissioned to investigate this application, as illustrated in Figure 1.

The heat is absorbed from the ground surrounding the GT in the ES and is transported by the CO_2 vapors to the HRV. Here, the cold IA is first pre-heated inside a plate-HE (HX-1) prior to its entry in the HRV where subsequent heat exchange between IA and EA occurs. This integration method does not require any external pumping loop to transport the (CO_2) heat transfer fluid (HTF).

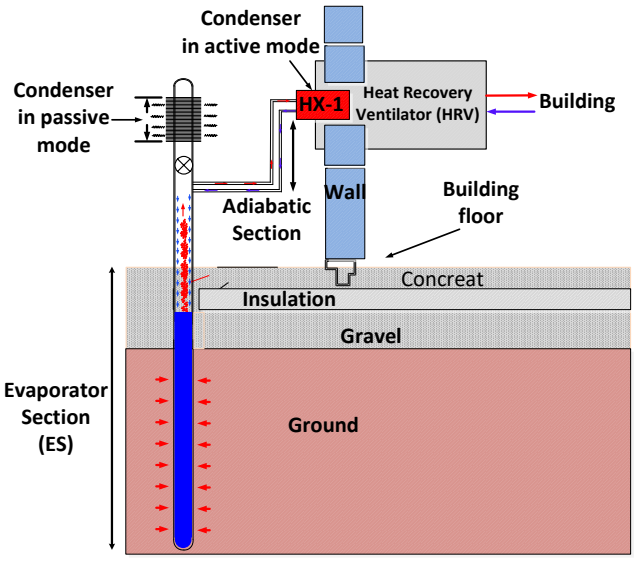

Fig. 1 Conceptual illustration of integrated of GT-HRV system.

Badache et al. (2024) evaluated the performance of the GT-HRV system under steady-state conditions. In continuation of this work, the objective of this study is to characterize the performance of the system during transient operation. This study specifically presents the results of the GT's transient response in terms of heat transfer rate, average evaporator temperature, and time constant.

2. EXPERIMENTAL METHODS

A fully instrumented experimental setup was commissioned to characterize the performance of GT as shown in Figure 2. The experimental setup has three loops: 1) Main HX-GT CO2 loop that simulates integration of HRV with GT 2) Propylene Glycol (PG) loop that acts as a buffer, and 3) R448a loop with a condenser unit to reject heat to the surrounding. PG loop and R448a loop provide precise control on the temperature of the PG to simulate test conditions for the main HX-GT loop.

Evaporator section of the GT (ES) consists of a 2 in. hollow stainless-steel tube, 30 m deep, filled with CO_2 and inserted into a casing consisting of a larger tube. The ES and the casing are thermally coupled with an HTF, and the assembly is buried in the ground. Thermophysical properties of the ground and HTF are provided in Table 1. Properties of the ground were determined using a thermal response test. ES is connected to an active condenser (HX-1) using ½ in steel pipes. The CO_2 vapors exit from the ES head and enter HX-1. Here, CO_2 transfers heat to the PG and changes phase from vapor to liquid under constant pressure. The CO_2 condensate exits the bottom of HX-1 under gravity. The condensate returns to the ES at an entry point located 0.3 m below the ES head.

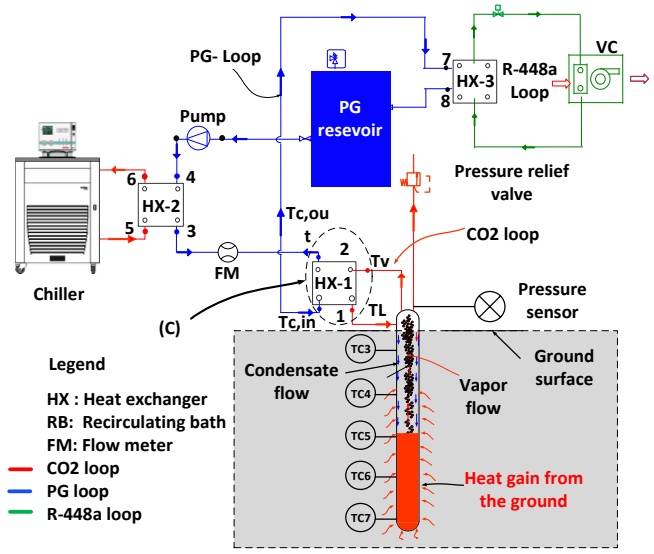

Fig. 2 Experimental test bench simulating integrated GT-HRV system.

Temperature data of the thermosyphon was captured using thermocouples located at 5 different locations on the surface of GT, at depths 3.05m, 9.14m, 15.24m, 21.33m and 27.43m. 40 plates, having an active surface area of 0.63 m^2, were available in the brazed plate HE (HX-1) and was fitted with RTDs on PG-HX-inlets and outlets. Their measurements were characterized by 0.15% uncertainty. Further details of the experimental setup can be found in our previous work (Badache et al. 2024).

Test runs were conducted for the GT filling ratio (FR) of 20% and thermal response was captured as temperature data located 5 seconds in time. The following test cases were simulated:

1. PG-HX inlet temperature ($T_{c,in}$) of -1 °C, -5 °C and -9°C were set and temperature response of ES TCs was captured for different flow rates.
2. PG loop flow rates of 0.05 l/s, 0.1l/s, 0.15 l/s and 0.2 l/s were simulated at all $T_{c,in}$ set points.

Selection of the test case parameters were made to comply with VDI 4640 guideline to limit the heat extraction to under 50 W/m for a sustainable geothermal energy extraction. When the temperature difference between PG inlet and the ground ($\Delta T_{g-T_{c,in}}$)is limited to the temperature range of 10-20 °C in the test conditions, the experimental simulation is representative of having average evaporator temperature ($T_{e,av}$) corresponding to mild/cold operating climatic conditions (-5 to 5 °C).

Heat transfer Fluid (HTF)		**Ground (g)**		
ρ_{HTF}	$c_{p\,HTF}$	**Conductivity**	$(\rho c_p)_g$	T_g
(kg/m^3)	(kJ/kg/K)	(W/m/K)	kJ/m^3/K	°C
1064.5	3720	2.65	2862	9.5

Table 1 Thermophysical properties of ground and HTF

3. THEORATICAL METHODS

This section summarizes the theoretical methods applied to characterize the performance of GT using the temperature data; in particular, heat transfer rate and time constant.

3.1. Heat transfer rate (Q)

The heat transfer rate of the GT can be estimated from the temperature measurements taken from the PG loop as all the energy extracted from the GT is dissipated in it. The total heat transfer rate at each time step is estimated using equation 1:

$$Q = \dot{m} Cp_c \rho_c (T_{c,out} - T_{c,in}) \quad (1)$$

Where ρ_c, Cp_c and $\dot{m}$ are the density, specific heat capacity and flow rates in the PG loop, respectively. $T_{c,out}$ and $T_{c,in}$ are the outlet and inlet temperatures, respectively.

3.2. Time Constant (T)

In an energy transport system, when a thermally capacitive element is combined with a thermally resistive element, the process can be characterized as a single time constant process (Tareen, M.S.K. 2017). In this experimental setup, the ground stores the heat and is treated as a thermally capacitive element while the thermal resistance is offered by the components of the experimental setup in the heat flow path from the ground to the PG loop. The time constant of such a system is determined by time taken for $\Delta T_{g\text{-}PG}$ (temperature difference between Ground and PG inlet) to reach 63.2% of the steady state value. The steady state of the temperature data in this study is defined as the average of the last 10 temperature values when the measurements are stabilized and do not fluctuate more than 0.2 °C in a 30-minute time frame. Time constant of the experimental data is calculated by using equation 2:

$$T(t) = T_f + (T_i - T_f) e^{-\frac{t}{\tau}} \quad (2)$$

Where, T_f and T_i are the average steady state final and initial values of the experimental data set. Value of T that best fits eq. 2 with the experimental data, by minimizing the error between both, is taken to be the time constant of the GT-HX energy transport system.

T characterizes the dynamic response of the system into a single parameter and can be used for various practical applications – particularly thermal response-based detection applications (Tareen M.S.K. 2017).

4. RESULTS AND DISCUSSION

This section provides the results of the transient response of GT in terms of heat transfer rate, average evaporator temperature and time constant for a subset of test cases specified in Section 2. The following results are presented:

a. Figure 3 illustrates the heat transfer rate over time for test case of FR of 20% and $T_{c,in}$ of -9 °C for all flow rates specified in Section 2.

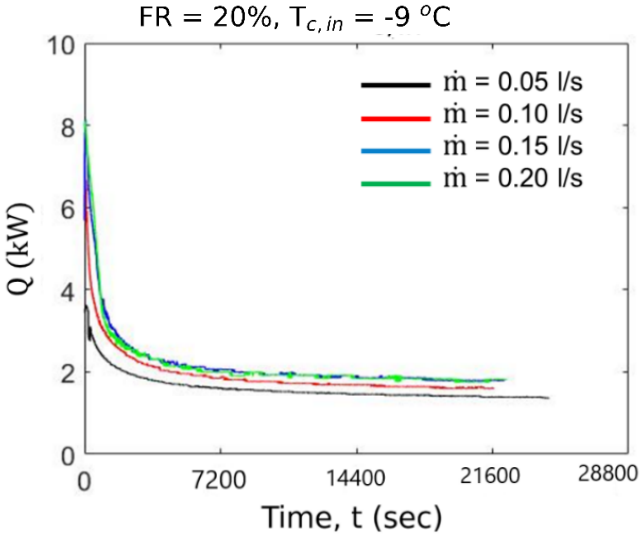

Fig. 3 Heat transfer rate from the GT to the PG loop.

b. Figure 4 illustrates the transient response of the GT in terms of average ES temperature for all test cases specified in Section 2. T_{ev} is the average of all five measurements of thermocouples (TC) taken at a particular time step. Location of each TC is defined in Section 2 and illustrated in the Figure 2.

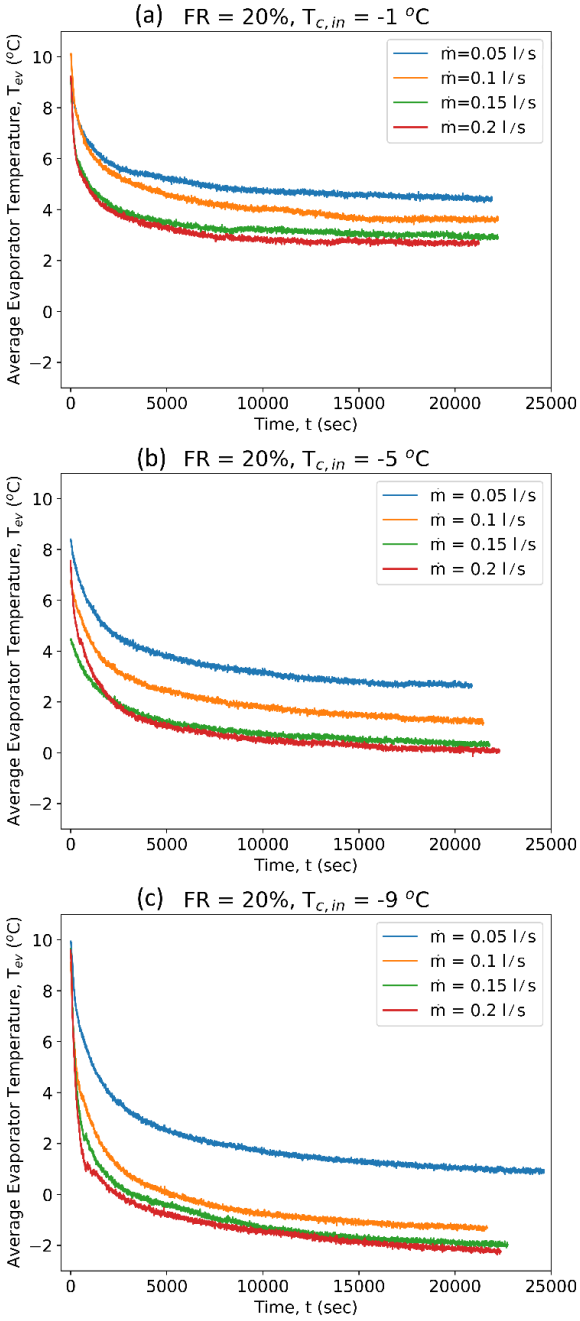

Fig. 4 Average evaporator temperature response for PG inlet temperatures of a) -1 °C, b) -5 °C and c) -9 °C

c. Figure 5 illustrates the time constants associated with thermal response curve of each test case specified in Section 2. Instead of presenting an average T for all five TCs, individual time constants for each TC level are presented.

Figure 3 illustrates a decrease in the heat transfer rate over time. This reduction can be attributed to the significant temperature difference between the circulating fluid and the ground temperature ($\Delta T_{g\text{-}PG}$) observed at the beginning of the GT operation. This temperature gradient results in higher initial heat transfer rates. For instance, the initial heat transfer rate (Q initial) is 8 kW at a flow rate of 0.2 l/s and 4 kW at a flow rate of 0.05 l/s. However, as the system continues to operate, ΔT_{g-PG} gradually diminishes due to the decrease in the ground temperature surrounding the GT, leading to a reduction in the heat transfer rate over time. As the system approaches steady state, the heat transfer rate stabilizes at a lower level. Like any heat exchanger, Figure 3 shows that high flow rates in the PG loop extract more heat from the ground at a faster rate compared to low flow rates, which extract less heat at a slower rate.

A steady state heat transfer rate of 2 kW presents a potential for integration of GT with HRV in cold regions. In addition of preserving the permafrost below the building of interest, the heat extracted from the ground will also reduce frost formation in the HRV. Energy is recycled without consuming additional energy that is typical of a conventional heat pump.

Thermal response of GT presented in the Figure 4 provides a novel validation reference for future numerical studies by researchers aiming to understand the boiling and condensation phenomenon of CO_2 inside GT.

High flow rate in the PG loop extracts heat at a faster rate compared to low flow rates that extract heat at a slower rate under same test conditions. This trend is observed in all three sets of results representing twelve unique cases reported in the figure 4. Consequently, the time constant is lowest at higher flow rates indicating relatively less time taken by the system to reach 63.2% of the steady state value of the temperature measurements. Higher PG flow improves convection heat transfer coefficient and reduces the resistance to heat transfer in the heat flow path.

Thermal response of GT is strongly dependent on $T_{c,in}$. It can be observed in Figure 4 and Figure 5 that lower $T_{c,in}$ corresponds to faster decay in the temperature reading as it enhances the condensation rate of CO_2 in the HX-1.

From Figure 5, it can be observed that there is a general trend of faster thermal response at the locations that are closer to the top of GT. TC 4 does not display this

behavior, most likely due to a systematic error. However, this trend is observed for TC-3, TC-5, TC-6 and TC-7 in the Figure 5a and 5c. The lowest location responds the slowest and thus has the highest time constant. This is expected because the lower we move along the ES, higher thermal resistance is offered by the progressively increasing mass of components of GT in the heat flow path.

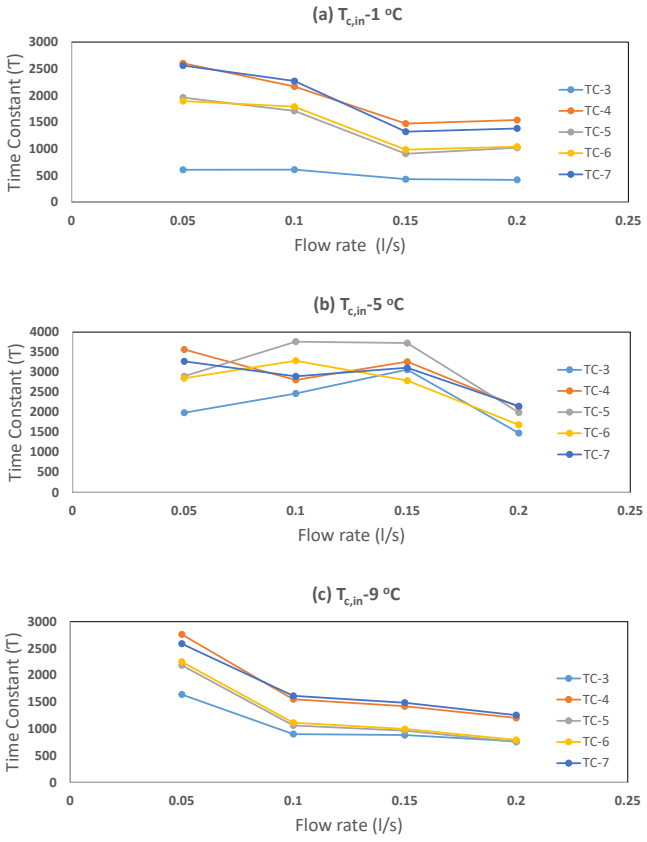

Fig. 5 Time constant associated with each TC level at all test cases: a) -1 °C, b) -5 °C, and c) -9 °C

It can also be speculated that the relatively colder condensate returning from the HX-1, trickling down along the ES walls, encounters the highest location first and further enhances the heat transfer rate at higher levels. At lower levels, the effect dampens as the temperature of the condensate return increases or mixes with the rest of the pool. Thus, a frozen body created around the GT-ES should have an inverted conical shape as experimentally validated in study conducted by Li et al (2020).

In figure 5(a) and 5(c) the trendlines are almost parallel indicating a directly proportional effect of depth on the thermal response. Higher flowrate of PG loop does not have a significant effect on the time constant if increased above 0.15 l/s. Deviations from this trend observed in the figure 5(b) may be due to limitations in the control loop where temperature was not precisely controlled in the test cases.

5. CONCLUSIONS

Overall, the transient thermal response of the GT is a measure of thermal resistance offered in the heat flow path. The transient response displays observable trends and is affected by flow rate and inlet temperature of PG. In addition, the thermal response along the depth of ES varies and displays a behavior consistent with the heat transfer principles. In such a single time constant process, provided all test conditions are kept the same, a change in thermal resistance, e.g. due to insulating frost film formation, can be detected by monitoring the time constant of the system. Integration of GT with HRV can thus be used with a dual intent: 1) to reduce frosting in HRV by pre-heating the IA, and 2) to detect the formation of the frosting layer on heat transfer surface of HRV. Further research is needed to qualify time constant of the thermal response curve as a detection method of frosting film in HRV in cold climates. Furthermore, work is in progress by the authors to characterize the transient performance of GT with different FRs.

ACKNOWLEDGEMENT

The first author would like to thank McGill Engineering Doctoral Award (MEDA) and FRQNT B2X award for funding the PhD studies. All the authors thank CanmetENERGY in Varennes, QC, CA for providing the financial and non-financial resources to carry out this research. The first and third author also acknowledge the funding contribution from Natural Sciences and Engineering Research Council of Canada (NSERC ALLRP 580457-22).

REFERENCE

[1] Badache, M., Aidoun, Z., & Manneh, F. (2024). A CO2 geothermal thermosiphon to preheat supply air for ventilation heat recovery systems in cold climates. Geothermics, 119, 102922. https://doi.org/10.1016/J.GEOTHERMICS.2024.102922

[2] Tareen, M. S. K. (2017). Heat Exchange Measurements During Initial Fouling Events (Master's thesis, State University of New York at Buffalo).

[3] Li, X., Li, J., Zhou, G., & Lv, L. (2020). Quantitative analysis of passive seasonal cold storage with a two-phase closed thermosyphon. Applied Energy, 260. https://doi.org/10.1016/J.APENERGY.2019.114250

[4] Mardiana-Idayu, A., & Riffat, S. B. (2012). Review on heat recovery technologies for building applications. In Renewable and Sustainable Energy Reviews (Vol. 16, Issue 2, pp. 1241–1255). https://doi.org/10.1016/j.rser.2011.09.026

[5] Mardiana, A., & Riffat, S. B. (2013). Review on physical and performance parameters of heat recovery systems for building applications. In Renewable and Sustainable Energy Reviews (Vol. 28, pp. 174–190). https://doi.org/10.1016/j.rser.2013.07.016

[6] Zhang, L., Song, M., Deng, S., Shen, J., & Dang, C. (2022). Frosting mechanism and behaviors on surfaces with simple geometries: A state-of-the-art literature review. In Applied Thermal Engineering (Vol. 215). Elsevier Ltd. https://doi.org/10.1016/j.applthermaleng.2022.118984

[7] Rafati Nasr, M., Fauchoux, M., Besant, R. W., & Simonson, C. J. (2014). A review of frosting in air-to-air energy exchangers. In Renewable and Sustainable Energy Reviews (Vol. 30, pp. 538–554). Elsevier Ltd. https://doi.org/10.1016/j.rser.2013.10.038

[8] Bai, H. Y., Liu, P., Justo Alonso, M., & Mathisen, H. M. (2022). A review of heat recovery technologies and their frost control for residential building ventilation in cold climate regions. In Renewable and Sustainable Energy Reviews (Vol. 162). Elsevier Ltd. https://doi.org/10.1016/j.rser.2022.112417